PIER Letters

(Received 1 Feburary 2024, Accepted 1 March 2024, Scheduled 7 March 2024)

A Dual-Port Pattern Diversity Antenna Based on FHMSIW Technology for Omnidirectional Coverage

Chu Zhang and Yangjun Ou*

School of Electronic Science and Engineering
University of Electronic Science and Technology of China (UESTC), Chengdu 611731, Sichuan, China

ABSTRACT: A dual-port pattern diversity antenna is proposed in this letter for omnidirectional coverage. Two end-fire radiating beams are realized based on a two-element magnetic current array. A folded half-mode substrate integrated waveguide (FHMSIW) is introduced to ensure that the distance between the two equivalent magnetic current radiation sources is about $\lambda_0/4$ (λ_0 is the wavelength in free space). When the two elements are driven by signals with a 90° or -90° phase difference, two end-fire radiation patterns with opposite directions can be realized. A prototype working at 2.425 GHz is fabricated and tested, achieving two independent end-fire radiation beams with a maximum gain of 4.3 dBi. Compared with conventional omnidirectional antennas, this work can effectively improve the gain of omnidirectional coverage based on a very compact structure.

1. INTRODUCTION

In the past decade, due to the continuous development of the Internet and Internet of Things technology, routers have become the core components of wireless local area network (WLAN) systems [1]. Routers typically use vertically polarized omnidirectional antennas [2, 3] and increase the gain on the horizontal plane by assembling arrays in the vertical direction [4–6], as shown in Fig. 1, while horizontally polarized omnidirectional antennas [7, 8] are easy to achieve a low profile, usually have a large disk profile, and are not suitable for router antenna applications. The space in the vertical direction is also limited by the external size of the product, and it is difficult to further improve the horizontal gain.

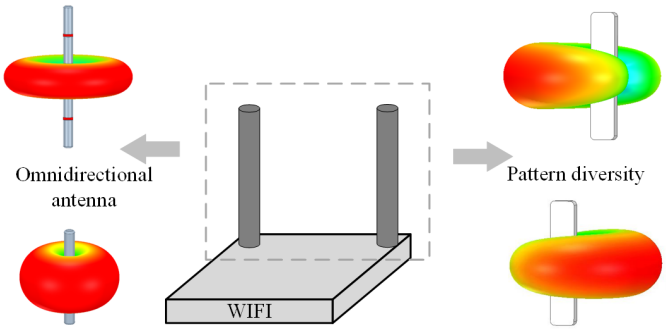

FIGURE 1. Different antenna schemes on the wireless router application.

As we all know, it is easier for directional antennas to achieve high gain performance than omnidirectional antennas. Covering the required space with higher antenna gain through two or more radiation beams is also the most attractive feature of pattern diversity antennas [9–14] and pattern-reconfigurable antennas [15, 16]. For router antenna application, it is feasible to improve the horizontal coverage gain by using the pattern diversity antenna, as shown in Fig. 1, but there are also challenges due to the special structure limitation.

At present, pattern diversity antenna is indeed a research hotspot, and most of the research focuses on improving the coverage of the antenna by using directional beam and conical beam [17–19], which is not suitable for realizing the omnidirectional coverage on a horizontal plane. For horizontal high-gain coverage, a few studies [20–22] discussed using multi-antenna techniques. For example, [20] proposes a scheme to achieve horizontal plane coverage using 6 beams, and the coverage gain also reaches 6–7 dBi. However, the essence of this scheme is that one beam corresponds to one directional antenna. Multiple directional antennas are combined into a ring array, resulting in a very large overall size and a complex feeding network.

To achieve directional radiation in a relatively compact space, complementary sources, such as magnetoelectric (ME) dipole antennas [23, 24] and Huygens Source antennas [25, 26], are candidate worth considering. Orthogonal magnetic dipole and electric dipole can realize a heart-shaped radiation pattern under suitable amplitude and phase excitation [23]. However, this radiation model requires that the M-dipole and E-dipole must be placed orthogonally for the back radiation zero, and vertical bar router antenna applications (Fig. 1) do not have such installation space.

The other way to achieve unidirectional radiation performance is based on end-fire array theory. Yagi dipole array [27, 28] is a classic case. With the evolution of antenna technology, magnetic current array end-fire antenna [29–31] as a more compact end-fire scheme has entered the stage. The achievement of the equivalent magnetic currents is mostly based on resonant cavities with open slots or open edges.

* Corresponding author: Yangjun Ou (yjouuestc@163.com).

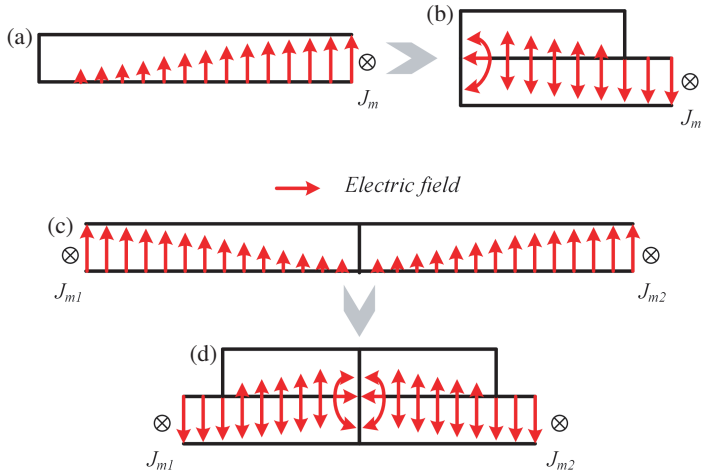

FIGURE 2. The schematic diagram of the HMSIW cavity and folded HMSIW cavity.

Thanks to its simple and efficient structure, the half-mode substrate integrated waveguide (HMSIW) [32] is a popular choice.

In this letter, a dual-port pattern diversity antenna based on a two-unit magnetic current array is proposed for omnidirectional coverage. The equivalent magnetic currents are realized by HMSIW cavities, and the two cavities share the shorting wall. Folded half-mode substrate integrated waveguide (FHMSIW) cavity technology is adopted for adjusting the cavity frequency while ensuring the spacing of the two elements keeping $\lambda_0/4$ (λ_0 is the wavelength in free space). A 90° 3-dB coupler bridge is made to drive the two elements with 90° phase difference signals. Two opposite end-fire radiation beams can be excited independently by the two input ports of the coupler bridge. The fabricated prototype works at 2.425 GHz. A radiation gain of 4.3 dBi with -15 dB cross-polarization is also investigated. The elongated structure ($0.22\lambda_0 \times 0.025\lambda_0 \times 0.57\lambda_0$) also supports arrays of antennas in the vertical direction to further improve the horizontal gain.

2. ANTENNA DESIGN

2.1. HMSIW and FHMSIW Cavity Array

Due to the low aspect ratio of the SIW cavity, if the standard SIW cavity is cut along a symmetry plane, the open side can be regarded as magnetic wall, and the modes of HMSIW cavity can remain stable compared to the original SIW cavity [33], so the typical width of the HMSIW cavity (Fig. 2(a)) is a quarter waveguide length (the size of the typical SIW cavity resonating in dominate mode is about 0.5×0.5 waveguide wavelength). However, one of the necessary conditions for obtaining a heart-shaped array factor is that the spacing between the two cells must be $\lambda_0/4$.

To achieve this purpose based on back-to-back HMSIW cavities (Fig. 2(c)), one way is to adopt the substrate with a high dielectric constant which can compress the waveguide wavelength, and the other way is to introduce a folded waveguide (Fig. 2(b)). The introduction of folded substrate-integrated waveguide (FSIW) technology can reduce the width of the HMSIW cavity by a maximum value of 50% with similar resonance characteristics to the original HMISW cavity [34]. The FHMSIW cavity provided an opportunity to simplify the antenna design procedure. We can regulate the spacing between the open edges of the HMSIW cavity (which can be regarded as the approximate radiation phase center of the equivalent magnetic current) to a quarter space wavelength (Fig. 2(d)), then adjust the resonant frequency by change the folded part of the HMSIW cavity.

The magnetic current radiation unit has omnidirectional radiation characteristics, so the realization of the end-fire radiation pattern mainly depends on the array factor. As shown in Fig. 3, by controlling the phase difference between the two magnetic current radiation sources to be $\pm 90°$, the antenna can be controlled to achieve two heart-shaped radiation patterns pointing opposite.

2.2. End-Fire Radiation

Since the FHMSIW technology offers the possibility to satisfy resonant frequency and element spacing simultaneously, a new FHMSIW model is chosen for a more compact structure. As shown in Fig. 4, the top-layer part of the FHMSIW cavity is shorter than the bottom-layer part, which is designed to reserve space for the feeding network. Placing two elements back-to-back and turning the width of the model to approximately $\lambda_0/4$, the radiation feature can be verified. The prerequisite for the principle of pattern multiplication (shown in Fig. 3) to work is that the single FHMSIW antenna should show an omnidirectional pattern in the horizontal plane. As shown in Fig. 5, when Prot_A and Prot_B are excited separately, the two units will exhibit similar omnidirectional radiation properties.

Figure 6 shows the radiation patterns when the two elements are fed by equal amplitude and different phases. A two-direction radiation characteristic (Fig. 6(a)) can be realized if the two elements are in-phase excited, while quasi-omnidirectional radiation (Fig. 6(b)) can be excited by driving the two elements out-of-phase. With feeding Port_A and Port_B with a 90° phase difference, unidirectional radiation

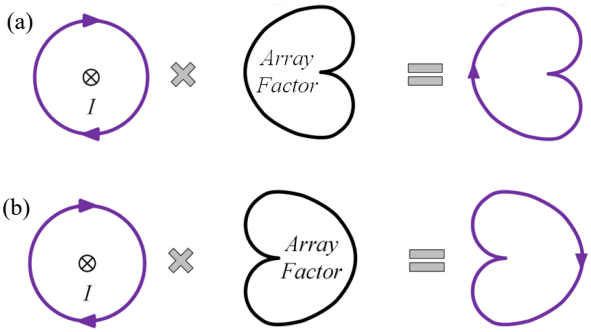

FIGURE 3. Different array factors realize different end-fire directions. (a) Left, (b) right.

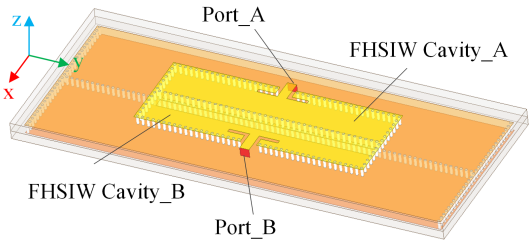

FIGURE 4. The configuration of the back-to-back FHMSIW cavity array.

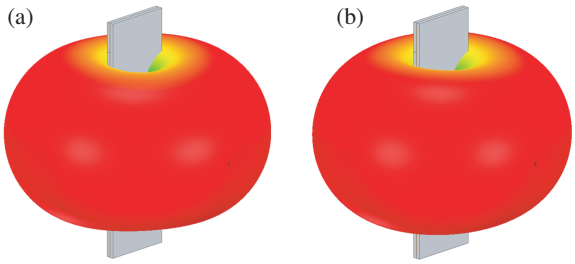

FIGURE 5. The radiation diagram for the magnetic current element. (a) Port_A excited, (b) Port_B excited.

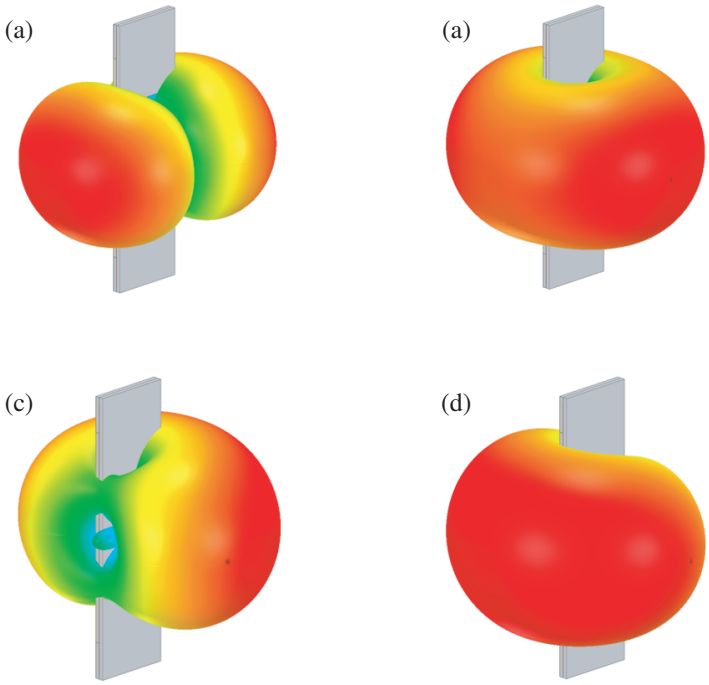

FIGURE 6. The radiation diagram for the two magnetic current elements with different excitation phases. (a) Common mode, (b) differential mode, (c) port_B lags port_A with 90° phase, and (d) port_A lags port_B with 90° phase.

feature can be observed. The beams are in opposite directions when element_I is 90° ahead excited and 90° lag. The two unidirectional radiation patterns (Figs. 6(c) and (d)) together can cover a space similar to the omnidirectional mode (Fig. 6(b)) with a higher gain.

A 90°-bridge based on microstrip lines can be integrated to stimulate the two-element array (Fig. 7). Due to the characteristics of the 90°-bridge, the two input ports (port_1 and port_2) are isolated while the two FHMSIW elements are driven with equal amplitude and 90° phase difference. According to the

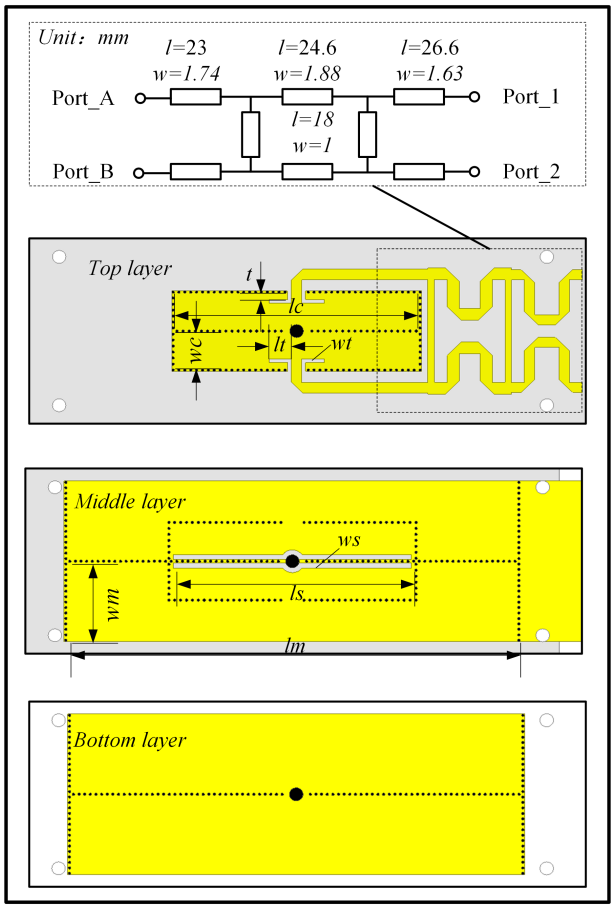

FIGURE 7. The configuration of the proposed dual-port pattern diversity end-fire antenna. $t = 1$ mm, $lc = 38$ mm, $lt = 3.5$ mm, $wt = 0.6$ mm, $wc = 5.9$ mm, $ws = 0.8$ mm, $ls = 37.6$ mm, $lm = 70$ mm, $wm = 12.8$ mm.

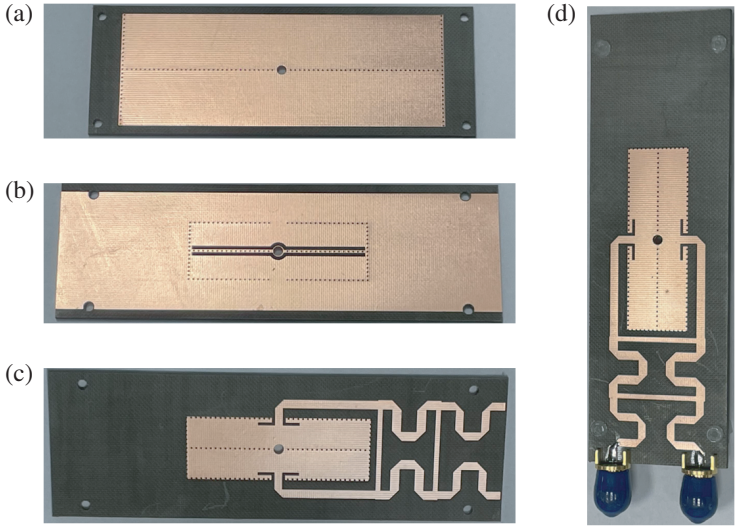

FIGURE 8. The photograph of the proposed dual end-fire beam antenna. (a) Bottom layer, (b) middle layer, (c) top layer, and (d) the overview of the proposed antenna.

previous analysis, Port_1 and Port_2 can drive two independent end-fire radiation beams with opposite directions.

3. EXPERIMENT

A prototype based on Fig. 7 is fabricated and tested. The upper and lower layer substrates are both the Taconic RF-35 with a dielectric constant $\varepsilon = 3.5$ and a same thickness of 1.52 mm. Thanks to the improved FHMSIW structure, the introduced feeding network can be coplanar integrated without an additional substrate layer. Photographs of the fabricated prototype are shown in Fig. 8. Two 50-Ω SMA connectors are soldered as the test ports.

3.1. Port Performance

Measured S-parameters are compared with the simulated results in Fig. 9, and a slight frequency shift can be observed. The working frequency of the antenna prototype is 2.425 GHz, meeting both the reflection coefficient standard ($|S_{11}| < -10$ dB) and port isolation standard ($|S_{21}| < -15$ dB). It can be seen that the $|S_{11}| < -15$ dB in a wide band, but the $|S_{21}|$ only exhibits good isolation in a narrow band. The antenna can only radiate energy when it is working in the band. Out of band means the electromagnetic energy will be coupled directly to the other port.

The bandwidth of this prototype is not very sufficient, mainly because the substrate thickness of 1.52 mm is only equivalent to $0.012\lambda_0$. The thin thickness makes the Q of the FHMSIW cavity very high, so the antenna bandwidth is limited. To a certain extent, increasing the thickness of the substrate can effectively improve the bandwidth. Simulation shows that if the substrate thickness is increased to 5 mm, the antenna bandwidth can be increased to 50 MHz (Fig. 9).

3.2. Radiation Performance

Figure 10 shows the simulated and measured antenna gains, the radiation performance of the prototype is obtained using a far-field test system. The measured maximum antenna gain is 4.3 dBi at 2.425 GHz, which has a certain gap with the simulated antenna gain. This phenomenon should also be attributed to the thickness of the substrate being too thin. High-Q cavity resonance makes the efficiency of the antenna very sensitive to the dielectric loss tangent of the substrate.

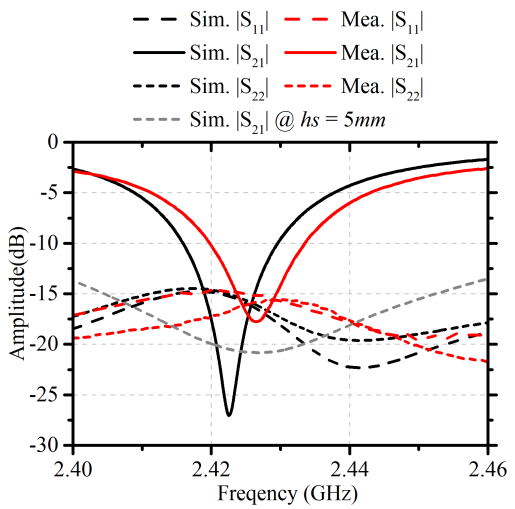

FIGURE 9. The S-parameters of the proposed dual end-fire beam antenna. (hs represents the thickness of the substrate).

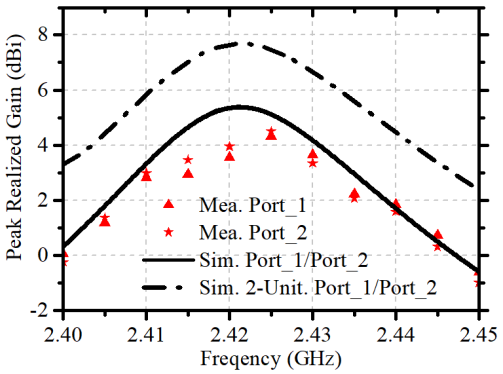

FIGURE 10. The simulated and measured gain of the proposed antenna.

TABLE 1. Comparisons with other router antennas.

Ref.	Radiation pattern	Structure	Pol.	Cross-section area (λ_0^2)*	Beam number	Band (GHz)	Peak gain (dBi)
[7]	Omni-direction	Circular platform	HP	1.00×0.06	1	1.6–2.6	3
[8]	Omni-direction	Circular platform	HP	3.3×0.04	1	3.8/5.3	1.5/0.8
[13]-ant1	Omni-direction	Circular platform	VP/HP	0.8×0.188	2	2.4/5.2/5.8	1/3**
[13]-ant2	Diversity	Circular platform	VP	0.8×0.188	2	2.4/5.2–5.8	0.06**
[14]	Diversity	Circular platform	VP	0.544×0.05	2	2.45	1.11**
[20]	Diversity	Circular platform	VP	0.55×2.2	6	5.5	7
This work	**Diversity**	**Vertical bar**	**HP**	$\mathbf{0.65 \times 0.024}$	**2**	**2.425**	**4.3/7.8*****

* λ_0 is the vacuum space wavelength in the lowest operating frequency.
** Specifically refers to omnidirectional mode radiation gain.
*** The gain of 7.8 dBi is a simulated result based on an array of 2 units in the vertical direction.

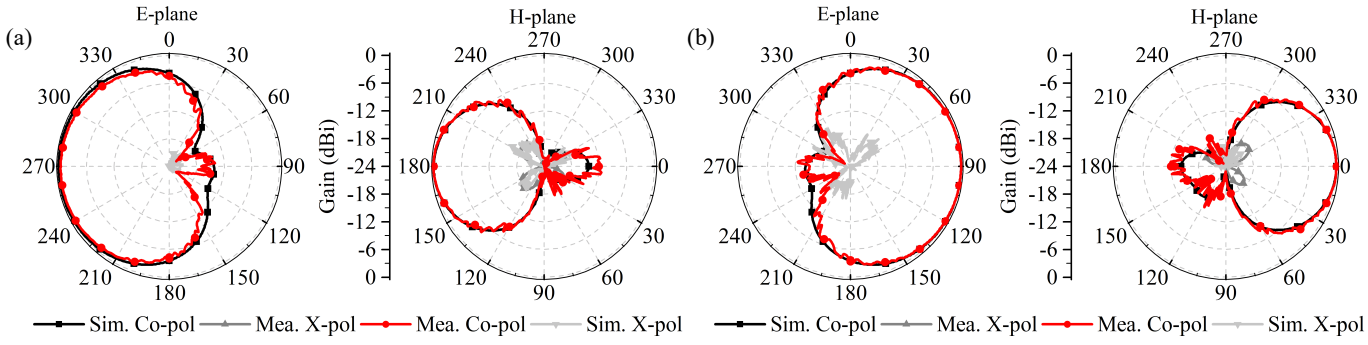

FIGURE 11. The normalized radiation pattern of the proposed dual endfire beam antenna by feeding. (a) Port_1 and (b) Port_2.

Figure 11 shows the measured radiation patterns compared with the simulated ones at 2.425 GHz in the E-plane (xoz-plane) and H-plane (yoz-plane). Two end-fire radiation patterns that point in opposite directions are visible. Measured radiation patterns show an FBR (front to back ratio) of 12 dB and a 15 dB cross polarization discrimination.

To highlight the main advantages of the proposed pattern diversity antenna method in the omnidirectional antenna design, a multidimensional comparison is conducted between the proposed antenna and previous router antennas (Table 1). The proposed antenna is the only multi-beam antenna based on a vertical bar shape. It achieves an advantageous horizontal coverage

gain. There is a margin for further array formation in the vertical direction to further increase the gain (Fig. 10).

4. CONCLUSION

In this letter, a new dual-port end-fire radiating antenna with pattern diversity is realized. The end-fire feature is achieved based on a two-element magnetic current array fed with equal amplitude and 90° phase difference. The two-element magnetic current radiation sources are equivalent to two FHMSIW cavities placed back-to-back. Two end-fire beams can cover the horizontal plane well. The design idea has been verified by fabricating and testing an antenna prototype. This compact vertical bar pattern diversity antenna provides a new perspective for the design of router antennas.

ACKNOWLEDGEMENT

This work was in part supported by the Advanced Functional Composite Technology Key Laboratory Fund under Grant Nos. 6142906220404 and Sichuan Provincial Central Guiding Local Science and Technology Development Project under Grant Nos. 2022ZYD0121.

REFERENCES

[1] Benyamina, D., A. Hafid, and M. Gendreau, "Wireless mesh networks design — A survey," *IEEE Communications Surveys & Tutorials*, Vol. 14, No. 2, 299–310, 2012.

[2] Chen, H.-D., "Compact broadband microstrip-line-fed sleeve monopole antenna for DTV application and ground plane effect," *IEEE Antennas and Wireless Propagation Letters*, Vol. 7, 497–500, 2008.

[3] Liu, W.-C., C.-M. Wu, and Y.-J. Tseng, "Parasitically loaded CPW-fed monopole antenna for broadband operation," *IEEE Transactions on Antennas and Propagation*, Vol. 59, No. 6, 2415–2419, Jun. 2011.

[4] Zhang, Y. and Y. Li, "Scalable omnidirectional dual-polarized antenna using cavity and slot-dipole hybrid structure," *IEEE Transactions on Antennas and Propagation*, Vol. 70, No. 6, 4215–4223, Jun. 2022.

[5] Chang, L., Y. Li, Z. Zhang, and Z. Feng, "Horizontally polarized omnidirectional antenna array using cascaded cavities," *IEEE Transactions on Antennas and Propagation*, Vol. 64, No. 12, 5454–5459, Dec. 2016.

[6] Zarifi, D. and A. Ahmadi, "An omnidirectional printed collinear microstrip antenna array," *Progress In Electromagnetics Research Letters*, Vol. 75, 33–38, 2018.

[7] Zhang, S. and M. Ye, "A wideband horizontally polarized omnidirectional antenna with coupling lines," *Progress In Electromagnetics Research Letters*, Vol. 62, 111–116, 2016.

[8] Zhang, H., D. Chen, Y. Yu, and C. Zhao, "A novel dual-frequency omnidirectional antenna with transmission line resonators loading," *Progress In Electromagnetics Research Letters*, Vol. 88, 43–50, 2020.

[9] Sun, L., G.-X. Zhang, B.-H. Sun, W.-D. Tang, and J.-P. Yuan, "A single patch antenna with broadside and conical radiation patterns for 3G/4G pattern diversity," *IEEE Antennas and Wireless Propagation Letters*, Vol. 15, 433–436, 2015.

[10] Liu, J., Z. Weng, Z.-Q. Zhang, Y. Qiu, Y.-X. Zhang, and Y.-C. Jiao, "A wideband pattern diversity antenna with a low profile based on metasurface," *IEEE Antennas and Wireless Propagation Letters*, Vol. 20, No. 3, 303–307, Mar. 2021.

[11] Bhattacharya, R., R. Garg, and T. K. Bhattacharyya, "A compact Yagi-Uda type pattern diversity antenna driven by CPW-fed pseudomonopole," *IEEE Transactions on Antennas and Propagation*, Vol. 64, No. 1, 25–32, Jan. 2016.

[12] Sun, L., W. Huang, B. Sun, Q. Sun, and J. Fan, "Two-port pattern diversity antenna for 3G and 4G MIMO indoor applications," *IEEE Antennas and Wireless Propagation Letters*, Vol. 13, 1573–1576, 2014.

[13] Hu, P. F., K. W. Leung, K. M. Luk, Y. M. Pan, and S. Y. Zheng, "Diversity glass antennas for tri-band WiFi applications," *Engineering*, Vol. 23, 157–169, 2023.

[14] Masood, R., C. Person, and R. Sauleau, "A dual-mode, dual-port pattern diversity antenna for 2.45-GHz WBAN," *IEEE Antennas and Wireless Propagation Letters*, Vol. 16, 1064–1067, 2016.

[15] Wang, R., B.-Z. Wang, G.-F. Gao, X. Ding, and Z.-P. Wang, "Low-profile pattern-reconfigurable vertically polarized endfire antenna with magnetic-current radiators," *IEEE Antennas and Wireless Propagation Letters*, Vol. 17, No. 5, 829–832, May 2018.

[16] Marantis, L., D. Rongas, A. Paraskevopoulos, C. Oikonomopoulos-Zachos, and A. Kanatas, "Pattern reconfigurable ESPAR antenna for vehicle-to-vehicle communications," *IET Microwaves, Antennas & Propagation*, Vol. 12, No. 3, 280–286, Feb. 2018.

[17] Yao, Y., J. Zheng, and Z. Feng, "Diversity measurements for on-body channels using a tri-polarization antenna at 2.45 GHz," *IEEE Antennas and Wireless Propagation Letters*, Vol. 11, 1285–1288, 2012.

[18] Fang, X. S., L. Luo, Y. J. Xu, and Z. Fan, "Design of the low-profile tri-polarized diversity cylindrical dielectric resonator antenna utilizing high-order $HEM_{13\delta}$ and $TM_{02\delta}$ modes," *IEEE Transactions on Antennas and Propagation*, Vol. 71, No. 11, 9060–9065, 2023.

[19] Zheng, Y., G. A. E. Vandenbosch, and S. Yan, "Low-profile broadband antenna with pattern diversity," *IEEE Antennas and Wireless Propagation Letters*, Vol. 19, No. 7, 1231–1235, 2020.

[20] Han, W., X. Zhou, J. Ouyang, Y. Li, R. Long, and F. Yang, "A six-port MIMO antenna system with high isolation for 5-GHz WLAN access points," *IEEE Antennas and Wireless Propagation Letters*, Vol. 13, 880–883, 2014.

[21] Wong, K.-L., Y.-R. Chen, and W.-Y. Li, "Eight-planar-monopole MIMO circular array generating eight uncorrelated waves for 6G upper mid-band 8×8 MIMO access points," *IEEE Access*, Vol. 11, 68 018–68 030, 2023.

[22] Wong, K.-L., Z.-W. Tso, and W.-Y. Li, "Very-wide-band six-port single-patch antenna with six uncorrelated waves for MIMO access points," *IEEE Access*, Vol. 10, 69 555–69 567, 2022.

[23] Luk, K.-M. and H. Wong, "A new wideband unidirectional antenna element," *International Journal of Microwave and Optical Technology*, Vol. 1, No. 1, 35–44, 2006.

[24] Luk, K.-M. and B. Wu, "The magnetoelectric dipole — A wideband antenna for base stations in mobile communications," *Proceedings of the IEEE*, Vol. 100, No. 7, 2297–2307, Jul. 2012.

[25] Ziolkowski, R. W., "Low profile, broadside radiating, electrically small huygens source antennas," *IEEE Access*, Vol. 3, 2644–2651, 2015.

[26] Tang, M.-C., T. Shi, and R. W. Ziolkowski, "A study of 28 GHz, planar, multilayered, electrically small, broadside radiating, huygens source antennas," *IEEE Transactions on Antennas and Propagation*, Vol. 65, No. 12, 6345–6354, Dec. 2017.

[27] Yagi, H., "Beam transmission of ultra short waves," *Proceedings of the IEEE*, Vol. 85, No. 11, 1864–1874, Nov. 1997.

[28] Brown, G. H., "Directional antennas," *Proceedings of the Institute of Radio Engineers*, Vol. 25, No. 1, 78–145, Jan. 1937.

[29] Liu, J. and Q. Xue, "Microstrip magnetic dipole Yagi array antenna with endfire radiation and vertical polarization," *IEEE Transactions on Antennas and Propagation*, Vol. 61, No. 3, 1140–1147, Mar. 2013.

[30] Yang, Z., L. Zhang, and T. Yang, "A microstrip magnetic dipole Yagi-Uda antenna employing vertical I-shaped resonators as parasitic elements," *IEEE Transactions on Antennas and Propagation*, Vol. 66, No. 8, 3910–3917, Aug. 2018.

[31] Liang, Z., Y. Li, J. Liu, S. Y. Zheng, and Y. Long, "Microstrip magnetic monopole endfire array antenna with vertical polarization," *IEEE Transactions on Antennas and Propagation*, Vol. 64, No. 10, 4208–4217, Oct. 2016.

[32] Deckmyn, T., S. Agneessens, A. C. F. Reniers, A. B. Smolders, M. Cauwe, D. V. Ginste, and H. Rogier, "A novel 60 GHz wideband coupled half-mode/quarter-mode substrate integrated waveguide antenna," *IEEE Transactions on Antennas and Propagation*, Vol. 65, No. 12, 6915–6926, Dec. 2017.

[33] Hong, W., B. Liu, Y. Wang, Q. Lai, H. Tang, X. X. Yin, Y. D. Dong, Y. Zhang, and K. Wu, "Half mode substrate integrated waveguide: A new guided wave structure for microwave and millimeter wave application," in *2006 Joint 31st International Conference on Infrared Millimeter Waves and 14th International Conference on Teraherz Electronics*, 219, Shanghai, China, Sep. 2006.

[34] Che, W., L. Geng, K. Deng, and Y. L. Chow, "Analysis and experiments of compact folded substrate-integrated waveguide," *IEEE Transactions on Microwave Theory and Techniques*, Vol. 56, No. 1, 88–93, Jan. 2008.